C. R. Physique 18 (2017) 118–124

Contents lists available at ScienceDirect

Comptes Rendus Physique

www.sciencedirect.com

Energy and radiosciences / Énergie et radioscience

Theoretical and practical limits of superdirective antenna arrays

Limites théoriques et pratiques des antennes superdirectives

Abdullah Haskou *, Ala Sharaiha, Sylvain Collardey

IETR UMR CNRS 6164, Université de Rennes-1, 263, avenue du Général-Leclerc, CS 74205, 35042 Rennes cedex, France

ARTICLE INFO

Article history:
Available online 5 December 2016

Keywords:
Superdirective antenna arrays
Parasitic elements
Theoretical and practical limits

Mots-clés :
Réseaux d'antenne superdirectifs
Éléments parasites
Limites théoriques et pratiques

ABSTRACT

Some applications as Wireless Power Transfer (WPT) require compact and directive antennas. However, Electrically Small Antennas (ESAs) have low efficiencies and quasi-isotropic radiation patterns. Superdirective ESA arrays can be an interesting solution to cope with both constraints (the compactness and the directivity). In this paper, the theoretical and practical limits of superdirective antennas will be presented. These limits can be summarized by the directivity sensitivity toward the excitation coefficients changes and the radiation efficiency decrement as the inter-element decreases. The need for negative resistances is also a practical limit for transforming these arrays into parasitic ones. The necessary trade-offs between the antenna total dimensions (the number of elements and the inter-element distance) and the attainable directivity and efficiency are also analyzed throughout this paper.

RÉSUMÉ

Certaines applications, comme le transfert d'énergie sans fil, nécessitent des antennes à la fois directives et compactes. Cependant, les antennes électriquement petites (AES) présentent de faibles rendements et des diagrammes de rayonnement quasi isotropes. Les antennes compactes superdirectives peuvent être une solution intéressante pour résoudre les problématiques concernant la directivité et l'efficacité énergétique. Dans cet article, nous présentons les limites théoriques et pratiques des antennes superdirectives. Ces limites sont le niveau de directivité en fonction de la sensibilité sur les coefficients d'excitation ainsi que la diminution de l'efficacité de rayonnement quand la distance inter-éléments diminue. Le besoin de résistances négatives pour concevoir des réseaux superdirectifs à éléments parasites est également une limite pratique dont il faut tenir compte. Les compromis nécessaires entre les dimensions totales de l'antenne (nombre des éléments et distance inter-éléments), la directivité et l'efficacité atteignables sont analysés dans cet article.

* Corresponding author.

http://dx.doi.org/10.1016/j.crhy.2016.11.003

1. Introduction

Many emerging radio technologies as the Internet of Things (IoT), wireless sensors, Wireless Power Transfer (WPT) and low-power wireless communications require a significant effort on the antenna miniaturization while keeping an acceptable performance (in terms of bandwidth, directivity, and efficiency). The effect of the antenna gain (efficiency and directivity) on far-field Power Transfer Efficiency (PTE) can be easily seen from the Friis transmission formula. Furthermore, Ick-Jae Yoon demonstrated that using directive antennas also improves the PTE in the near-field region [1]. However, antenna performance is limited, with some fundamental limits related to its physical dimensions. Multiple researchers addressed the fundamental limits of Electrically Small Antennas (ESAs) [2–6]. A.H. Wheeler defined an ESA as an antenna with $ka < 1$, where $k = \frac{2\pi}{\lambda}$ is the wave number, λ is the free-space wavelength and a is the radius of the smallest sphere enclosing the antenna [2]. Due to these fundamental limits, ESAs are characterized by their narrow bandwidths, their quasi-isotropic radiation patterns (radiating energy in non-desired directions) and their low efficiencies (high power consumption). These characteristics will lead to a considerable loss in the link budget, and, as a consequence, small communications ranges. To increase the directivity of ESAs, one can integrate them in arrays. However, the conventional arrays (where the inter-element distance is around half a wavelength) lead to a significant increase in their size. At the same time, since the pioneering work of I. Uzkov [7], there has been a renewed interest in superdirective arrays (the inter-element distance is set to a small fraction of the wavelength) [8–18]. While decreasing the distance increases the attainable directivity, it also increases the mutual coupling, hence it can have a considerable effect on the array efficiency.

In [17], we detailed the design procedure of small parasitic superdirective arrays. In this paper, the theoretical and practical limits of superdirective antennas will be presented. The necessary trade-offs between the antenna overall dimensions, the attainable directivity and efficiency will be detailed. This analysis is validated via the full-wave simulation and the measurement of a three-element array.

The rest of the manuscript is organized as follows: superdirective antenna limits are discussed in section 2. The results are validated via the design of a three-element array in section 3. Finally, conclusions are drawn in section 4.

2. Theoretical limits of superdirective arrays

Consider an array of antennas located at positions r_n, $n = 1, 2, \ldots, N$ with respect to a fixed rectangular (xyz) coordinate system. The complex far field radiated by the array in (θ, ϕ) is given by:

$$f(\theta,\phi) = \sum_{n=1}^{N} A_n f_n(\theta,\phi)\, \mathrm{e}^{\mathrm{j}k\hat{r}r_n} \tag{1}$$

where A_n are the complex excitation coefficients, $f_n(\theta,\phi)$ are the complex radiated far fields and $\hat{r}$ is the unit vector in the far-field direction (θ,ϕ). The array directivity is given by:

$$D(\theta,\phi) = \frac{|f(\theta,\phi)|^2}{\frac{1}{4\pi}\int_0^{2\pi}\int_0^{\pi} |f(\theta,\phi)|^2 \sin(\theta)\,\mathrm{d}\theta\,\mathrm{d}\phi} \tag{2}$$

The Uzkov–Altshuler current excitation coefficients that maximize the directivity in the direction (θ_0,ϕ_0) are given by [7,8]:

$$a_{0n} = [H^*_{mn}]^{-1}\mathrm{e}^{-\mathrm{j}k\hat{r_0}r_m} f^*_m(\theta_0,\phi_0) f_n(\theta_0,\phi_0) \tag{3}$$

where $\hat{r_0}$ is the unit vector in the far field direction (θ_0,ϕ_0), and H_{mn} is given by:

$$H_{mn} = \frac{1}{4\pi}\int_0^{2\pi}\int_0^{\pi} f_m(\theta,\phi) f^*_n(\theta,\phi)\mathrm{e}^{\mathrm{j}k\hat{r}(r_m - r_n)} \sin(\theta)\,\mathrm{d}\theta\,\mathrm{d}\phi \tag{4}$$

Now let us consider an array of N isotropic radiators equally spaced by a distance d along the z axis with the first element located in the coordinate system origin. The calculated excitation coefficients of three- and four-element arrays are given in Figs. 1 and 2. These excitation coefficients reveal that, for an array of a fixed number of elements, high excitation magnitudes are required for small distances, and, as the distance increases, the excitation magnitude decreases. For $d = 0.5\lambda$ all the excitation magnitudes are equal. It can be noticed that the symmetric elements (1,2 for $N = 2$, 1,3 for $N = 3$, 1,4, and 2,3 for $N = 4$) have equal excitation magnitudes. It can also be noticed that for a fixed spacing, increasing the number of elements significantly increases the excitation magnitudes. By applying these excitation coefficients, the maximum directivity that can be obtained as a function of the inter-element distance is given in Fig. 3(a). It may be noticed that when the distance between the elements approaches zero, the array directivity approaches N^2. Increasing spacing decreases the directivity in the main direction and increases it in the backward direction (Fig. 3(b)). At 0.5λ, the directivity in both end-fire directions is equal to N (refer to Fig. 3(c)). Fig. 3(d) shows the power radiated by the array for power-normalized excitation coefficients, i.e. $(\sum_{n=1}^{N} A_n^2 = 1)$. This power is calculated as follows:

E-mail address: abdullah.haskou@univ-rennes1.fr (A. Haskou).

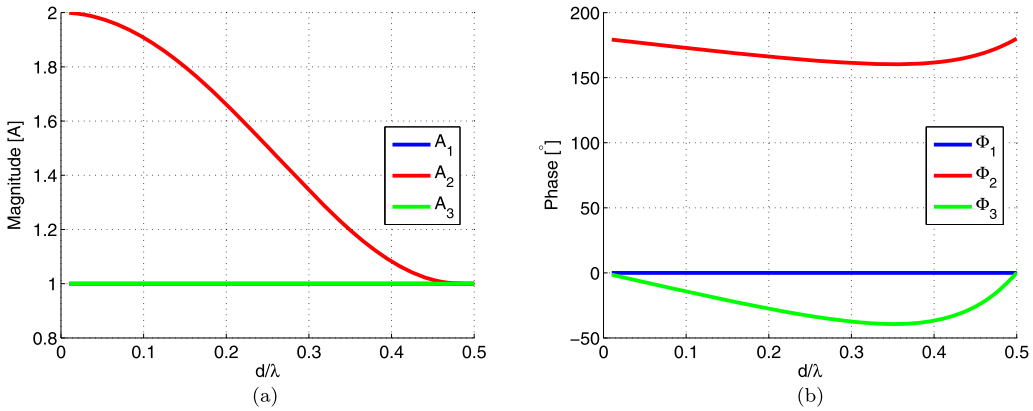

Fig. 1. Three d-spaced isotropic array optimal excitation coefficients. (a) Magnitude and (b) phase.

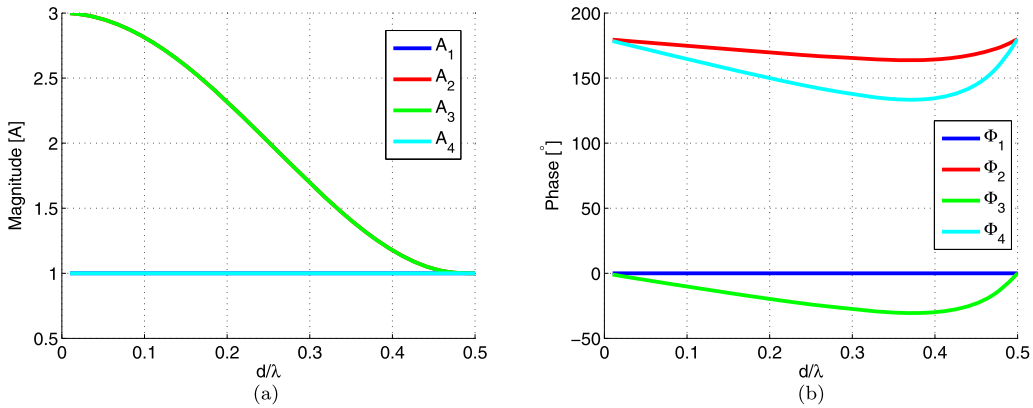

Fig. 2. Four d-spaced isotropic array optimal excitation coefficients. (a) Magnitude and (b) phase.

$$P_{\text{rad}} = \frac{1}{2} \oiint_S \text{Re}(E \times H^*)\, \text{d}s \approx \frac{1}{2\eta} \oiint_S |E|^2 \text{d}s \approx \frac{1}{2\eta} \int_0^{2\pi} \int_0^{\pi} |E|^2 r^2 \sin(\theta)\, \text{d}\theta\, \text{d}\phi \tag{5}$$

where η is the intrinsic impedance of the medium (air), r is the radius of the sphere over which the radiated power is calculated, and E is the total far-field electric field and can be calculated as in Eq. (1). We can notice that, for the same distance, as the number of the elements increases, the radiated power decreases, and, as a consequence, so does the array radiation efficiency. To study the sensitivity of the array toward the excitation coefficients, we re-calculated the directivity when the coefficients magnitudes are estimated with an error of 5% or the phases are shifted by 5°. Fig. 4 shows the obtained results (since the symmetric elements have equal magnitudes, the array sensitivity toward the errors in these elements' excitation is also the same, so they are not shown). It may be noted that, for small spacing, the array is very sensitive to the changes in the coefficients. It is also possible to notice that, for a fixed distance, increasing the number of the elements increases the array sensitivity. For a distance $d = 0.1\,\lambda$, an error of 5% in the estimation of the first element's magnitude reduces directivity by 1.1%, 10.2%, or 56.1% in case of an array of two, three, or four elements, respectively. It is also observed that, for an array of N elements, the array is more sensitive to the changes in the coefficients of the middle elements. This is due to the fact that the magnitudes of these coefficients are higher. After presenting the theoretical limits of superdirective arrays, we will show in the next section some practical limits via the design of a three-element array.

3. Design of a three-element array

The superdirective antenna array design methodology detailed in [17] was used to design a three-element array. The unit-element used in this array is a miniaturized half-loop antenna printed on a 0.8-mm-thick Rogers RO4003 substrate and integrated in a PCB of 8×8 cm^2 [18]. It has a resonance frequency around 864 MHz with a directivity of 2.4 dBi and a radiation efficiency of 89.4%. The proposed antenna geometry is shown in Fig. 5(a). The inter-element distance d_1 is varied from 0.69 cm $\approx 0.02\,\lambda$ to 6 cm $\approx 0.17\lambda$ to investigate its effect on the antenna's maximum directivity and radiation efficiency. Fig. 5(b) shows the array directivity compared to Harrington's fundamental limit on the directivity of an antenna with the same size ka given by $D = (ka)^2 + 2ka$ [6]. As expected, it can be noticed that for very small distances, the

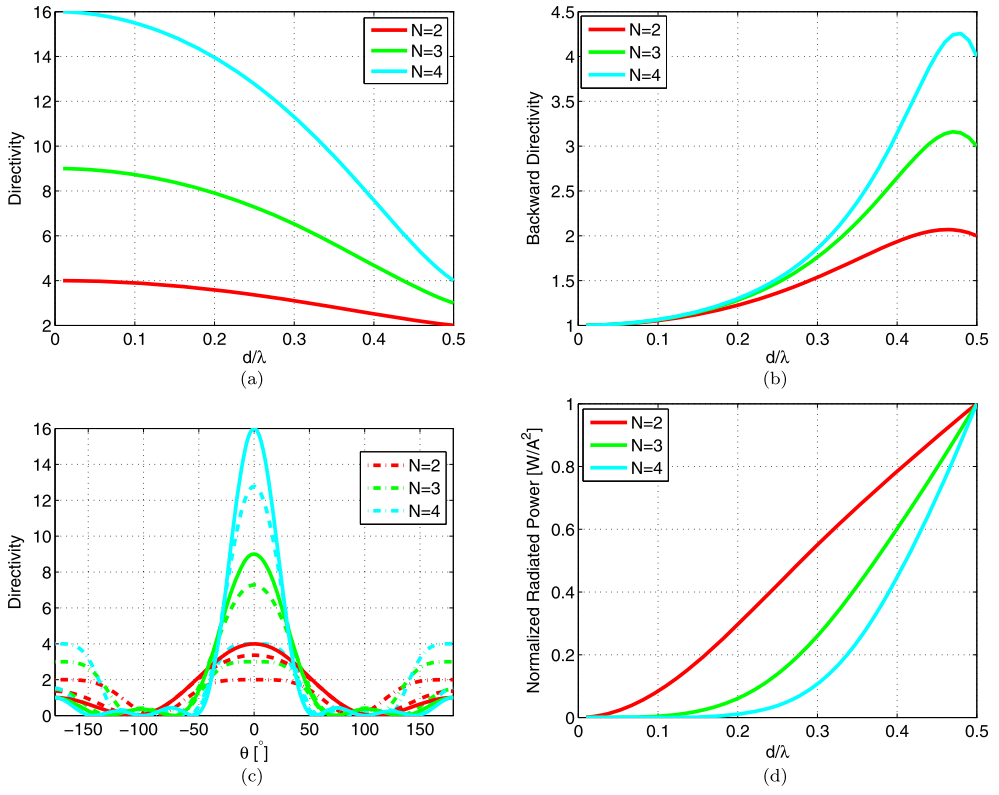

Fig. 3. The performance of N-element d-spaced isotropic array. (a) Directivity in the main end-fire direction, (b) directivity in the backward end-fire direction, (c) 2D total directivity radiation pattern for $d = 0.01$ (continuous), $d = 0.25$ (dashed), and $d = 0.01$ (dashed–dotted), and (d) normalized transmitted power.

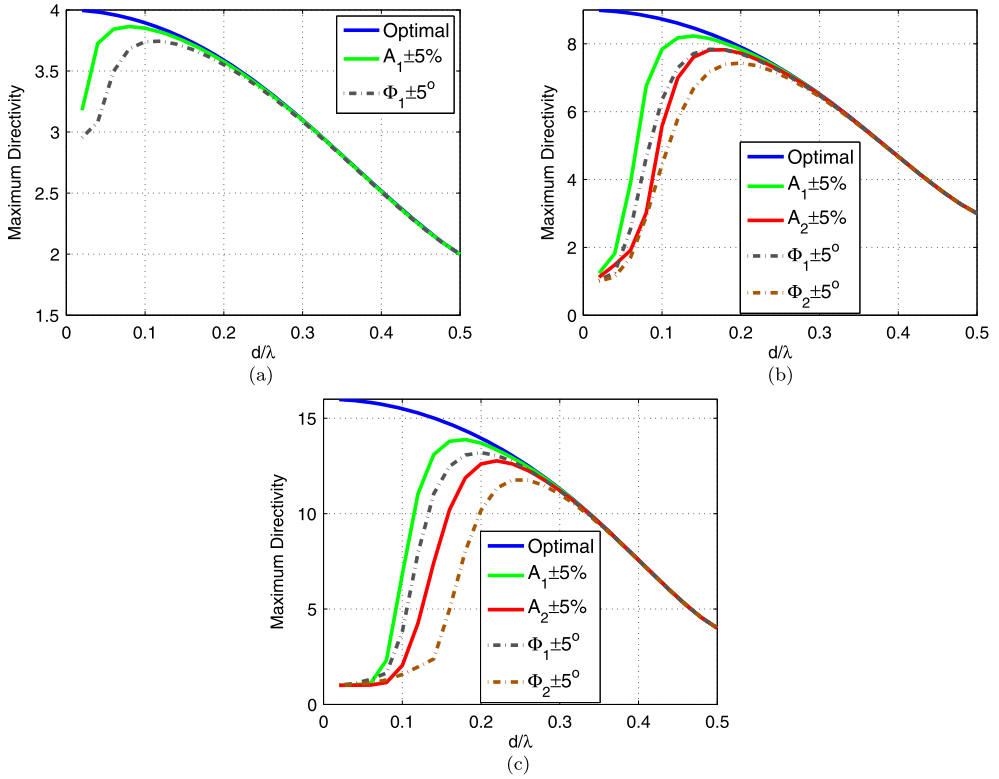

Fig. 4. The effect of the error in the coefficients estimation on the directivity of N-element d-spaced isotropic array. (a) $N = 2$, (b) $N = 3$, and (c) $N = 4$.

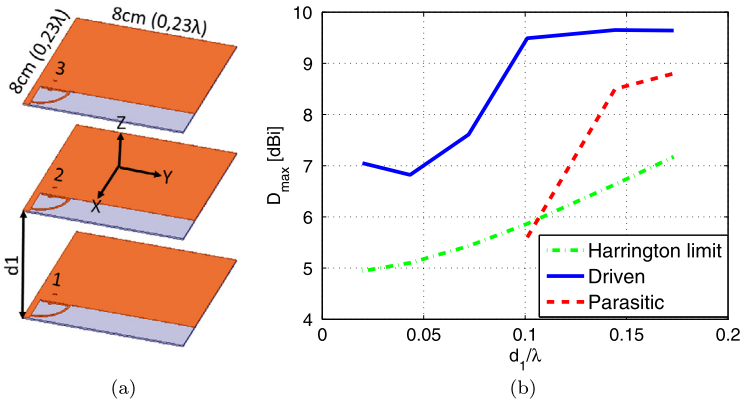

Fig. 5. Proposed superdirective array. (a) Array geometry and (b) simulated total directivity.

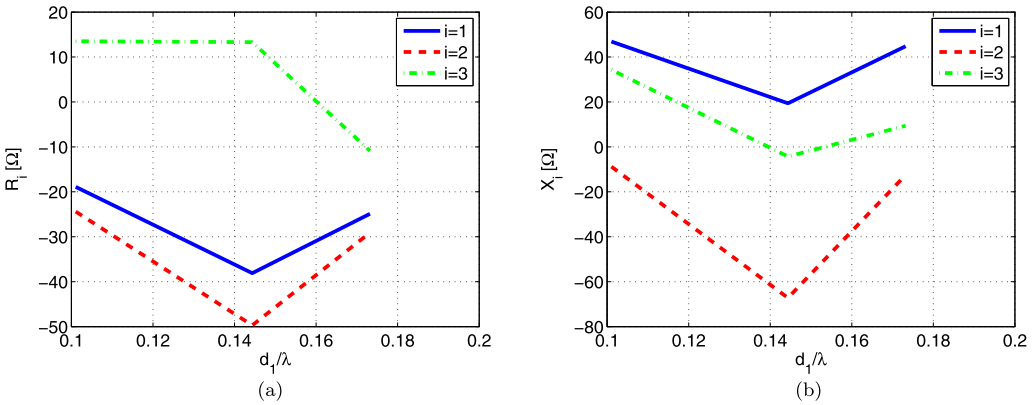

Fig. 6. The value of the required loads for converting the array into a parasitic one. (a) Real part and (b) imaginary part.

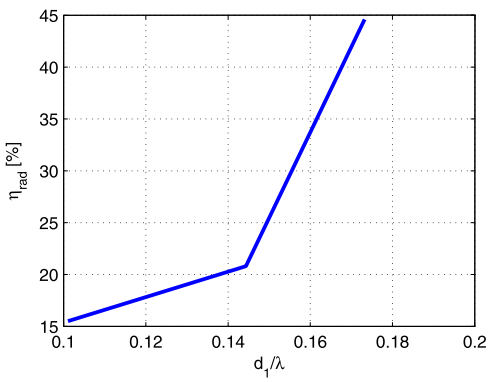

Fig. 7. Parasitic array simulated radiation efficiency.

driven array is very sensitive to the excitation coefficients, and a small error in the calculation of these coefficients leads to an important decrement in the antenna's directivity. As distance increases, this sensitivity decreases and, starting from $d_1 = 3.5$ cm $\approx 0.08\lambda$, interesting directivity values can be attained. The value of the required loads for transforming the array into a parasitic one is given in Fig. 6. As it can be noticed, some negative resistances are required, and since the design of negative resistances using non-Foster circuits is not an easy task, neglecting these resistances significantly decreases the attained directivity compared to the fully driven array. Finally, Fig. 7 shows that, as expected due to the coupling decrement, the parasitic array radiation efficiency increases with the inter-element distance. A prototype of the antenna array for $d_1 = 6$ cm $\approx 0.17\,\lambda$ was fabricated and measured (Fig. 8(a)). In this array, the second element is excited, while the others are loaded. Fig. 8(b) shows the antenna input reflection coefficient magnitude in dB. As it can be noticed, the antenna has a simulated/measured resonance at 863/868 MHz with a $S_{11} < -10$ dB bandwidth of 1.7/5 MHz. The higher losses in the measurement may be attributed to the UFL cable used for measurement. Fig. 8(c) shows the antenna's 3D total directivity

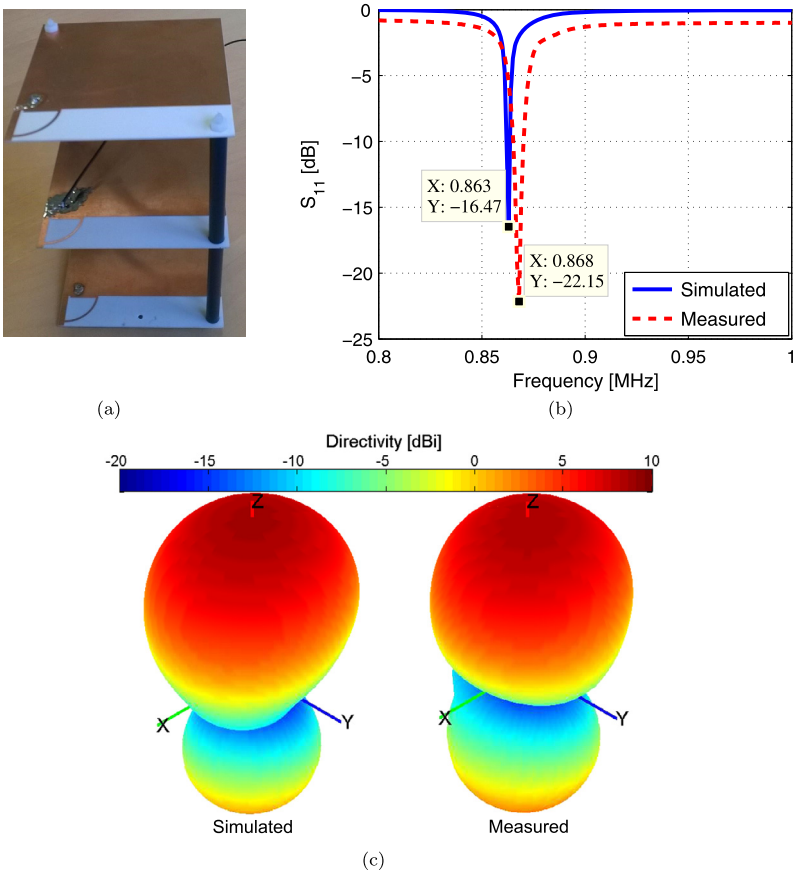

Fig. 8. Simulated and measured parameters corresponding to a three-element array with 6-cm spacing. (a) Fabricated prototype, (b) input reflection coefficient magnitude in dB, and (c) 3D total directivity radiation pattern.

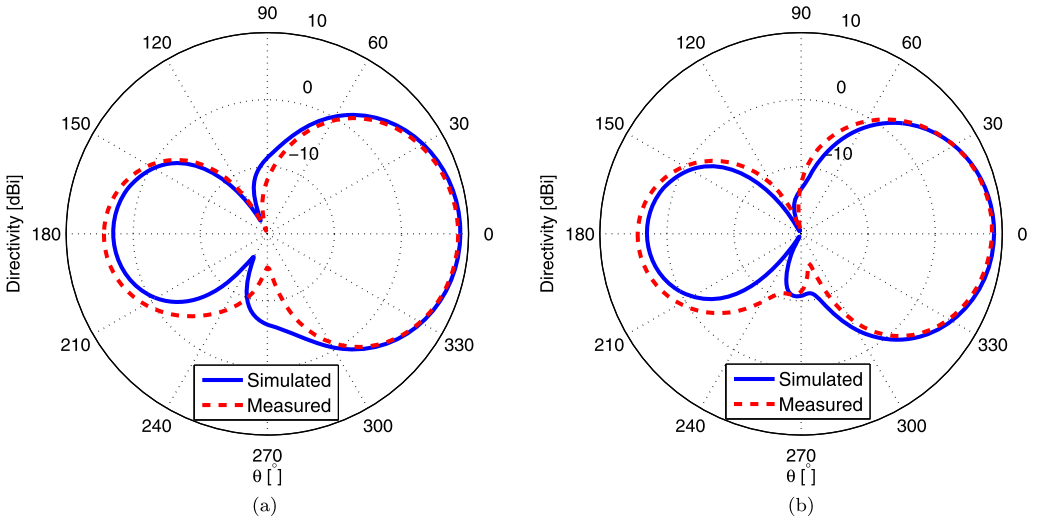

Fig. 9. Simulated and measured parameters corresponding to 2D total directivity radiation patterns for a three-element array with 6-cm spacing. (a) E-plane, (b) H-plane.

radiation pattern. The figure shows a directive pattern with a directivity of 8.8/8.5 dBi toward the z-axis. This directivity is larger by about 1.4 dB than Harrington's normal directivity limit for an antenna with the same size factor ($ka = 1.6$). The HPBWs in the E (XoZ) and H (YoZ) planes are, respectively, 72°/73.1° and 64°/67.5°, and FBR is 5.8 dB/4.1 dB (Fig. 9). The antenna presents a radiation efficiency of 34.7%/37%.

4. Conclusion

In this article, we have shown the theoretical and practical limits of the design of superdirective antenna arrays. These limits can be summarized by the array's sensitivity to excitation coefficients and the small efficiencies for very closely spaced arrays, and the need for negative resistances for transforming the arrays into parasitic ones. In general, the design of superdirective antenna arrays is a trade-off between the antenna dimensions (the number of elements and the inter-element distance) and the attained directivity and efficiency. Superdirective and efficient arrays can be designed through a careful consideration of these trade-offs.

Acknowledgements

This work has been funded by the French National Research Agency (ANR-11-INFR-014) as part of the project "SOCRATE", and with the support of the "Images et réseaux" cluster of the Brittany region, France.

References

[1] I.-J. Yoon, Realizing Efficient Wireless Power Transfer in the Near-Field Region Using Electrically Small Antennas, PhD dissertation, The University of Texas at Austin, TX, USA, 2012, available at: http://hdl.handle.net/2152/ETD-UT-2012-08-6167.
[2] H.A. Wheeler, Fundamental limits of small antennas, Proc. IRE 35 (12) (1947) 1479–1484.
[3] H.A. Wheeler, The radiansphere around a small antenna, Proc. IRE 47 (8) (1959) 1325–1331.
[4] L.J. Chu, Physical limitations of omni-directional antennas, J. Appl. Phys. 19 (12) (1948) 1163–1175.
[5] R.M. Fano, Theoretical limitations on the broadband matching of arbitrary impedances, J. Franklin Inst. 249 (1) (1950) 57–83, J. Franklin Inst. 249 (2) (1950) 139–154.
[6] R.F. Harrington, On the gain and beamwidth of directional antennas, IRE Trans. Antennas Propag. 6 (3) (1958) 219–225.
[7] I. Uzkov, An approach to the problem of optimum directive antennae design, C. R. (Dokl.) Acad. Sci. URSS 53 (1) (1946).
[8] E.E. Altshuler, et al., A monopole superdirective array, IEEE Trans. Antennas Propag. 53 (8) (2005) 2653–2661.
[9] T.H. O'Donnell, A.D. Yaghjian, Electrically small superdirective arrays using parasitic elements, in: IEEE Trans. Antennas Propag. Soc. Int. Symp., 9–14 July 2006, pp. 3111–3114.
[10] T.H. O'Donnell, et al. Frequency optimization of parasitic superdirective two element arrays, in: IEEE Trans. Antennas Propag. Soc. Int. Symp., 9–15 June 2007, pp. 3932–3935.
[11] S. Lim, H. Ling, Design of electrically small Yagi antenna, Electron. Lett. 43 (5) (2007) 3–4.
[12] A.D. Yaghjian, et al., Electrically small supergain end-fire arrays, Radio Sci. 43 (2008), http://dx.doi.org/10.1029/2007RS003747.
[13] O.S. Kim, et al., Superdirective magnetic dipole array as a first-order probe for spherical near-field antenna measurements, IEEE Trans. Antennas Propag. 60 (10) (2012) 4670–4676.
[14] B. Sentucq, et al. Superdirective compact parasitic array of metamaterial-inspired electrically small antenna, in: Proc. 2013 International Workshop on Antenna Technology, iWAT, Karlsruhe, Germany, 4–6 March 2013, pp. 269–272.
[15] M. Pigeon, et al. Miniature and superdirective two elements endfire antenna array, in: Proc. 8th European Conference on Antennas and Propagation, EuCAP 2014, The Hague, The Netherlands, 6–11 April 2014, pp. 6–11.
[16] A. Clemente, et al., Design of a super directive four-element compact antenna array using spherical wave expansion, IEEE Trans. Antennas Propag. 63 (11) (2015) 4715–4722.
[17] A. Haskou, et al., Design of small parasitic loaded superdirective end-fire antenna arrays, IEEE Trans. Antennas Propag. 63 (12) (2015) 5456–5464.
[18] A. Haskou, et al. Compact planar arrays based on parasitic superdirective elements, in: Proc. 10th European Conference on Antennas and Propagation, EuCAP 2016, Davos, Switzerland, 10–15 April 2016.